Research Article

Toward Sustainable Composites: Comparative Performance of Natural and Synthetic Fibers under Low-Velocity Impact

Ravi Sevak* and Nihaal Jamdar
Mechanical Engineering Program, School of Engineering and Technology, Navrachana University, Gujarat, India

* Corresponding author. E-mail: ravis@nuv.ac.in DOI: 10.14416/j.asep.2025.11.009
Received: 18 June 2025; Revised: 21 August 2025; Accepted: 6 October 2025; Published online: 20 November 2025

Abstract

This research presents a novel computational–experimental framework for comparing synthetic and natural fibers in low-velocity impact scenarios to advance environmentally friendly alternatives to synthetic composites. Uniquely, microwave-assisted compression-molded ramie/HDPE composites were fabricated and experimentally tested to validate Mori–Tanaka predictions of elastic modulus, achieving close agreement before transferring the homogenized properties to finite element impact simulations. The study examines synthetic fibers such as Kevlar, carbon fiber, and S-glass alongside natural fibers including hemp, flax, ramie, and jute, all within a High-Density Polyethylene (HDPE) matrix, across fiber mass fractions of 10–30%. Results highlight the promise of natural fibers, particularly ramie, which showe d a consistent rise in force reaction from 0.25 kN at 10% to 2.0 kN at 30%, positioning it as a strong candidate for reinforcement, stiffness, and thermal stability. Among synthetics, carbon fiber maintained steady performance with a force reaction of 0.45 kN at 10–20% and 0.75 kN at 30%, while also exhibiting the least deformation at higher fractions, underscoring its reliability for high-performance applications. These findings confirm the feasibility of integrating natural fibers into composite materials as sustainable substitutes, while providing a balanced benchmark against established synthetic fibers. The proposed validated multiscale methodology opens new directions for eco-conscious material design in automotive, construction, and related industries.

Keywords: Finite element simulation, Hemp, Low velocity impact, Natural fiber composites, Sustainability

1 Introduction

From wood in the early 10,000 BC to metals in the 1900s, the world is moving towards high-strength, low-weight materials, wherein polymer composites are playing a vital rôle [1]. These materials are made of two distinct phases: the matrix and the fiber. The fiber medium is the central pillar of all the properties of the composite material, whereas the matrix is the phase that holds the entire composition together and helps distribute the load [2], [3]. Fibers have also undergone substantial improvements in the last few decades and can be divided into synthetic and natural categories. Synthetic fibers are man-made fibers that undergo chemical processes during manufacturing. These most commonly include glass fibers, carbon fibers, etc. Synthetic fibers are not limited to just these; steel bars have been used as a suitable fiber material in tandem with FRP laminates to ultimately make up a composite material, and have been studied for their mechanical properties [4], [5]. Even nanotubes, such as carbon nanotubes and boron nitride nanotubes, have also been used as a fiber material with HDPE as a matrix for composites to be studied under low-velocity impact [6], [7]. Although effective in achieving high performance, synthetic reinforcements remain energy-intensive, costly, and environmentally challenging to recycle, thereby limiting their sustainability.

Contrary to synthetic fibers, natural fibers are not man-made; they are derived from nature, either from animals or plants [8]. Natural fibers such as hemp, flax, and jute are some of the most commonly used natural fibers [9]. Physical properties of sisal fiber-based composites, such as impact strength and tensile

and flexural strength with different orientation methods, have been studied to check their compatibility to potentially replace synthetic fibers [10], [11].

Natural fiber composites offer several advantages over synthetic fiber composites. One significant advantage is their environmental sustainability [12]. Natural fibers, sourced from plants like hemp, flax, and jute, are renewable resources, reducing dependence on non-renewable materials. Additionally, natural fibers are biodegradable, contributing to eco-friendly disposal practices [13], [14]. Another benefit is that the lower production energy required for natural fibers than synthetic ones results in a reduced carbon footprint. Natural fiber composites also exhibit good thermal insulation properties, making them suitable for specific applications. However, compared to synthetic fibers like carbon or Kevlar, natural fibers often exhibit lower tensile strength and stiffness and are more prone to moisture absorption, leading to reduced dimensional stability [15], [16]. Additionally, natural fibers display variability in properties due to species, harvesting, and processing conditions, making consistency in composite performance a significant challenge [15]. Thus, while natural fibers provide clear environmental benefits, their mechanical limitations and variability restrict their widespread adoption in high-performance applications.

The performance evaluation of the composites can be done experimentally and computationally. Before the computerized simulation, analytical methods, such as the rule of mixtures, were mainly used by researchers to determine the properties of composite materials, such as strength, stiffness, and thermal conductivity, based on the mass fractions or the volume fractions [17], [18]. Later on, molecular dynamics was introduced as a computer-aided simulation that predicted the movement of the atoms or the molecules of the composite material to give a detailed atomic-level understanding of the material's behavior subjected to different operational conditions [19].

The current study focuses on using computer-powered simulations to establish the behavior of materials when they undergo a low-velocity impact. Hufenbach *et al*., performed a study that focused on comparing experimental results with the simulated results using glass fiber as reinforcement with epoxy and polypropene as matrix materials. The simulated target was subjected to a drop test tower, and experimental and computational results were compared, which were found to agree with each other [20]. Zyu *et al*., studied low-velocity impact with differently oriented targets. The study presented a validated analytical model for analysing the low-velocity impact response of foam core sandwich panels with composite face sheets. The model accurately predicts force-displacement curves, peak load, impactor displacement, failure patterns, damage area, and energy absorption, aligning well with experimental observations. The investigation into energy partition reveals that deformation energy dominates in composite face sheets. In contrast, the plastic strain energy of the core significantly influences energy absorption in the entire sandwich panel. This research provides valuable insights into impact failure mechanisms and energy absorption, offering a robust analytical approach for designing composite sandwich panel configurations [21]. Narayana *et al*., conducted the study based on introducing a contact relation for lightweight sandwich panels, considering the impact of local membrane stretching in face sheets. A linear expression approximates the force-indentation relation for small face sheet indentation depths relative to the core thickness. Based on quasi-static and dynamic behaviours, analytical models were developed using this contact relation to calculate impact force during low-velocity impacts on circular sandwich panels. The model's validity hinges on the mass ratio (m) between the colliding projectile and the effective sandwich plate mass. A quasi-static model suffices for large mass ratios ($m > 8$), especially when deflection is substantial compared to panel thickness. Conversely, if the mass ratio is small ($m < 8$), modal superposition becomes crucial for accurately predicting dynamic responses. The study emphasizes the importance of suitable material models for sandwich core simulations, highlighting that residual indentation depends on maximum impact force, influenced by panel size, structural properties, projectile mass, and striking energy [22].

While prior research has yielded significant insights into the behavioral impact of composites, the majority has focused on either synthetic fiber systems, which provide enhanced mechanical performance but lack sustainability, or on natural fiber composites that are environmentally advantageous yet constrained in strength and durability. Moreover, most studies depend solely on either computational modeling or experimental testing, with minimal integration of both, thereby constraining the capacity for valid, evidence-based comparisons within shared matrices. Due to escalating environmental concerns, there is heightened interest in replacing synthetic fibers with

biodegradable natural alternatives, including hemp, flax, ramie, jute, and kenaf. These natural fibers diminish reliance on non-renewable resources while providing benefits such as biodegradability, recyclability, and reduced energy consumption in production, therefore aiding worldwide initiatives for eco-friendly and sustainable material practices. Notwithstanding this promise, the literature remains deficient in comprehensive studies that directly juxtapose natural and synthetic fibers under low-velocity impact within an integrated computational-experimental framework. This research examines the possibilities of natural fiber composites as alternatives to synthetic systems, thereby enhancing scientific knowledge and promoting sustainable engineering solutions. In particular, there is a shortage of research that integrates microwave-assisted composite fabrication, substantiation of homogenization techniques such as Mori–Tanaka, and finite element modeling of low-velocity impacts within a unified framework.

This work is driven by applications involving structural components exposed to low-velocity impact loading, including vehicle interior and exterior panels, protective casings, building materials, and lightweight consumer products. These sectors require materials that harmonize mechanical performance, impact resistance, and sustainability, rendering natural fiber composites a viable substitute for synthetic reinforcements.

2 Materials and Methods

2.1 *Mori-Tanaka homogenization method and its mathematical background*

The elastic behavior of composites has been micromechanically predicted using standard models, such as the law of mixtures. They connect the characteristics of the components that make up fiber composites to their stiffness. The elastic modulus of such composites has upper and lower bounds given by Equations (1) and (2), and their Poisson's ratio can be found using Equation (3). Nevertheless, they are not very precise since they ignore heterogeneities, such as fiber orientation and form.

$$E_c = V_f . E_f + \left(1 - V_f\right). E_m \quad (1)$$

$$E_c = \frac{V_f}{E_f} + \frac{(1-V_f)}{E_m} \quad (2)$$

$$\vartheta_c = V_f . \vartheta_f + \left(1 - V_f\right). \vartheta_m \quad (3)$$

The current study uses the Mori-Tanaka method to evaluate the properties of composites. The Mori-Tanaka homogenization scheme is a theoretical approach used to estimate the effective mechanical properties of composite materials, particularly those consisting of a continuous matrix phase with embedded inclusions or reinforcements. This method offers a means to predict the overall behavior of the composite by considering the mechanical interactions between the matrix and inclusions. The Mori-Tanaka approach assumes a two-phase composite consisting of a homogeneous matrix and dispersed inclusions. The inclusions within the matrix can have different shapes, sizes, and orientations. The key idea is to establish relationships between the local field (within the individual inclusions) and the overall or macroscopic properties of the composite. The method involves averaging the local fields to derive effective macroscopic properties. The homogenization process begins by defining local fields within the inclusions, such as stress or strain. These local fields are then averaged over the composite volume to obtain the macroscopic or effective properties. The method incorporates the orientation and volume fraction of the inclusions, considering their distribution and arrangement within the matrix. The Mori-Tanaka homogenization scheme is beneficial for predicting composites' effective stiffness and thermal conductivity. It applies to a range of composite materials, including those with isotropic or anisotropic constituents. However, it assumes that the inclusions are slight compared to the overall size of the composite, allowing for a statistically representative volume element. The assumptions taken in the Mori Tanaka method are 1) fibers are uniformly distributed and modeled as aligned ellipsoidal inclusions, 2) perfect interfacial bonding exists between the fiber and matrix, 3) the matrix is considered linear elastic and isotropic, 4) fiber–fiber interactions are disregarded, and 5) the surrounding matrix is treated as infinite in extent. These assumptions facilitate analytical tractability and are reasonable at low to moderate fiber fractions. However, they may restrict accuracy at very high fractions, where interaction effects become substantial.

Eshelby [23] first presented an analytical method for homogenization in 1957. He devised a technique to calculate the stiffness matrix that involved taking it out of the RVE, letting it reshape, and then applying a surface force to bring it back into the matrix. The macro-scale fields, when averaged over the matrix and inclusion phases, can be expressed as a volumetric average shown in Equation (4):

$$\{\blacksquare\} = (1 - V_f)\{\blacksquare\}_m + \sum_{j=1}^{n} V_f^j \{\blacksquare\}_j \quad (4)$$

The stress field inside the inclusion is related to the mismatch in strain between the matrix and inclusion through the fourth-order tensor X_{ijkl}, as given in Equation (5):

$$\sigma_{ijkl} = X_{ijkl}(\epsilon_1 - \epsilon_2) \quad (5)$$

Finally, the strain concentration relation between the inclusion and matrix phases can be expressed in terms of the concentration tensor Yi_{jkl}, as shown in Equation (6):

$$\epsilon_1 = Y_{ijkl}\,\epsilon_2 \quad (6)$$

where ϵ_1 and ϵ_2 are proportional to each other by a fourth-order Y_{ijkl}The tensor, known as Eshelby's Tensor, is a second-order strain transformation tensor for both limited and unconstrained inclusions.

For ellipsoidal inclusions in a homogeneous matrix, Y_{ijkl} is a constant. For an elliptic cylinder with semi-major and minor axes of x and y, Eshelby's tensor is given by [23].

The normal strain components along the principal axes are given in Equations (7)–(9):

$$Y_{1111} = \frac{1}{2(1-\nu)}\left[\frac{y^2+2xy}{(x+y)^2} + (1-2\nu)\frac{y}{x+y}\right] \quad (7)$$

$$Y_{2222} = \frac{1}{2(1-\nu)}\left[\frac{x^2+2xy}{(x+y)^2} + (1-2\nu)\frac{x}{x+y}\right] \quad (8)$$

$$Y_{3333} = 0 \quad (9)$$

The coupling strain components between different directions are provided in Equations (10)–(12):

$$Y_{1122} = \frac{1}{2(1-\nu)}\left[\frac{y^2}{(x+y)^2} - (1-2\nu)\frac{y}{x+y}\right] \quad (10)$$

$$Y_{2233} = \frac{\nu x}{2(1-\nu)} \quad (11)$$

$$Y_{3311} = Y_{3322} = 0 \quad (12)$$

The shear-related terms are expressed in Equations (13)–(16):

$$Y_{1212} = \frac{1}{2(1-\nu)}\left[\frac{x^2+y^2}{(x+y)^2} - \frac{(1-2\nu)}{2}\right] \quad (13)$$

$$Y_{1133} = \frac{\nu y}{(1-\nu)(x+y)} \quad (14)$$

$$Y_{2323} = \frac{x}{2(x+y)} \quad (15)$$

$$Y_{3131} = \frac{y}{2(x+y)} \quad (16)$$

This idea was further upon by Mori Tanaka in 1973 [23] by extending it to RVEs with numerous inclusions of similar shapes.

2.2 *Materials*

In the present work, high-density polyethylene (HDPE-50MA180) powder purchased from Reliance Chemicals (Mumbai, India) was used as matrix material with natural fiber reinforcement to create a unidirectional mat of ramie (200 GSM). The properties of both materials are listed in Table 1. (Supplier: Fiber region, Chennai, India)

Table 1: Mechanical properties of matrix and reinforcement.

Properties	High-Density Polyethylene	Ramie
Young's Modulus (GPa)	3.2	128
Poisson's ratio	0.3	0.3
Density (g/cm^3)	0.95	1.5

2.3 *Fabrication and testing*

The novel technique of microwave-assisted compression molding was used for the fabrication of natural fiber composites. An alumina mold of size 90 × 25 × 20 mm^3 was used to fabricate the composites. Unidirectional ramie mats were layered between layers of HDPE powder to prepare the composites. The mass of HDPE powder used to create each composite was selected to maintain a consistent mass fraction of natural fiber in all the composites. To fabricate composites, the alumina mold with the teflon fixture was put in the microwave applicator at the appropriate microwave power and processing time. The fabrication setup used to fabricate the composites is shown in Figure 1. Pilot runs were used to determine the amount of microwave power and processing time needed to produce the composites. The composites were fabricated with 10%, 20%, and 30% mass fractions of fibers. To optimize the microwave power and the processing time, Experiments were performed at microwave power levels of 300, 450, 600, and 750 W. At 300 W and 450 W, HDPE exhibited no melting or only partial melting after 780 seconds, inhibiting composite production. At 600 W, a processing duration of 650 ± 40 s was deemed appropriate for the softening of HDPE and the successful manufacturing of composites. Conversely, 750 W resulted in excessive heating, which produced fiber combustion and compromised the composites. Consequently, 600 W with a processing window of 650 ± 40 s was

determined to be the best setting for composite manufacturing, following which the samples were extracted and visually examined. The fabricated composites are shown in Figure 2. After fabrication, the composite specimens were subjected to the tensile test at a crosshead speed of 1 mm/min in accordance with ASTM D3039. Table 2 shows the Young's modulus values of the composite specimen. The scanning electron microscopy of the tensile fractured surfaces was used to understand the distribution of fiber and matrix fiber bonding. Figure 3 shows the scanning electron microscope image of the fractured surface of the composite under tensile loading. The image shows that the HDPE matrix is tightly bonded with ramie fibers. The fractured surface reveals matrix and fiber elongation, indicating a strong matrix-ramie fiber connection, which indicates the greater load transfer between ramie fibers and HDPE matrix. The fractured section also shows the uniform distribution of the fibers through the entire cross-section.

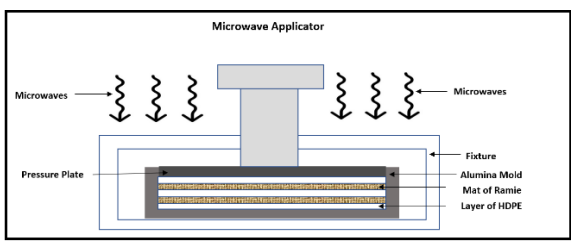

Figure 1: Set up used for the microwave-assisted compression molding of composites

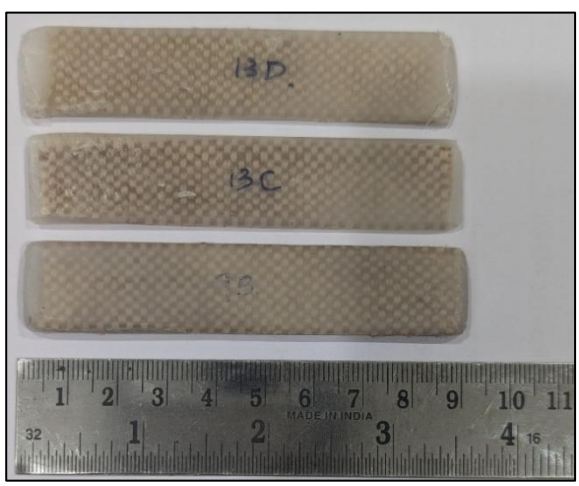

Figure 2: Composites fabricated by microwave-assisted compression molding.

2.4 *Experimental and computational validation*

The experimental results obtained after tensile testing and the values obtained after Mori-Tanaka homogenization are compared in Table 2. The experimental values are validated with the computational method by 10 % variation, which shows that both methods agree with each other, and the computational values of properties can be used to do the low-velocity impact analysis for various natural and synthetic fiber composites. The variation seen between the simulated and actual values of Young's modulus can be attributed to several factors inherent in the modeling assumptions and material properties. An essential factor is the interfacial bonding strength between the fiber and matrix, often idealized in analytical models, although it can significantly fluctuate in real composites due to inadequate adhesion, voids, or weak chemical interactions. Research reveals that insufficient interfacial bonding can impair load transfer efficiency, hence decreasing the effective modulus of the composite [24]. Another key influence is the orientation and distribution of fibers inside the matrix. The Mori-Tanaka and Double Inclusion models assume uniform and aligned fiber orientations; however, natural fiber composites often exhibit random or semi-aligned orientations due to processing techniques, leading to diminished stiffness in experimental samples compared to the idealized models [25]. Furthermore, the variation in fiber length, aggregation, and moisture content in natural fibers may enhance the diversity in mechanical performance. Incorporating micromechanical models that account for defective bonding and stochastic fiber orientation may improve the accuracy of predictive simulations in future studies.

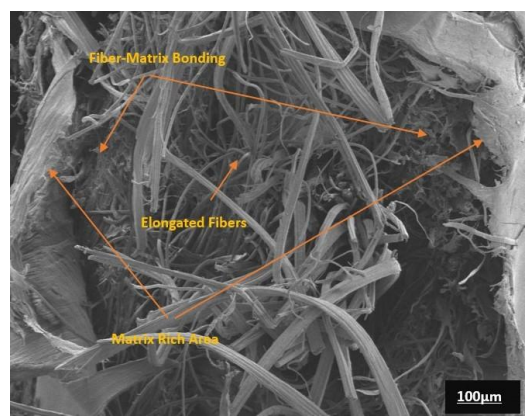

Figure 3: Scanning electron microscope image of tensile fractured HDPE/Ramie composite.

Table 2. Validation of the computational model with the present experimental analysis.

Mass Fraction of Ramie (M_f)	Experimental Modulus (GPa)	Modulus predicted by Mori Tanaka Homogenization (GPa)
0.1	10.15 ± 1.4	11.405
0.2	18.4 ± 2.1	20.259
0.3	28.2 ± 2.4	29.843

2.5 *Properties of composites*

The preceding section has shown that the mechanical properties assessed by the homogenization approach agree with experimental data. As a result, in the following sections, mechanical properties are evaluated where the fiber structure is relatively complex, and the values are challenging to determine empirically by utilizing computational homogenization approaches. The natural and synthetic fibers considered in the current study are listed in Table 3. All the fibers are considered to be continuous and unidirectional in nature. Fibers are considered to have an aspect ratio greater than the critical value of the aspect ratio.

Table 3: Properties of fibers under study [8].

Fiber	Density (g/cm^3)	Young's Modulus (GPa)	Poisson Ratio
Hemp	1.5	70	0.4
Flax	1.5	80	0.45
Ramie	1.5	128	0.3
Jute	1.5	55	0.375
Kevlar	1.44	131	0.35
S-Glass	2.55	87	0.22
Carbon Fiber	1.4	240	0.28

A comparison of the axial Young's modulus for various natural fiber composites made by applying the Mori-Tanaka homogenization method is presented in Figure 4. It is noticeable that Ramie composites have a higher Young's modulus than other natural fiber composites for the same volume percentage. Ramie fibers' greater stiffness is the reason for this. A similar observation can also be drawn for the In-plane Young's modulus. Using the Mori Tanaka homogenization method, Figure 5 compares the axial Young's modulus of the three synthetic fiber composites. It is noticeable that carbon fiber composites have a greater Young's modulus than other natural fiber composites for the same volume percentage. This is explained by the increased rigidity of carbon fibers. One can also make a comparable observation regarding In-Plane Young's modulus.

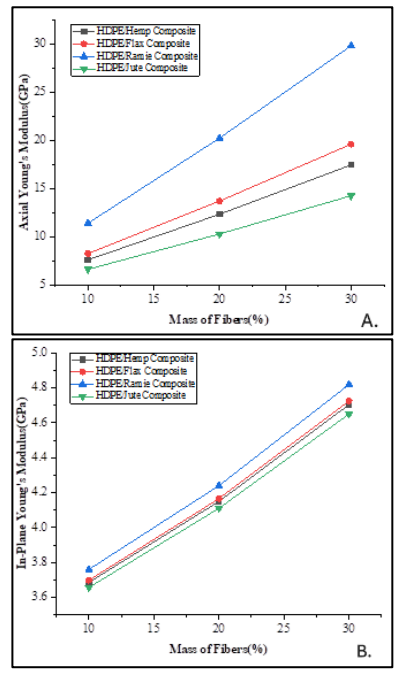

Figure 4: Comparison of (A) axial Young's modulus and (B) In-plane Young's modulus for different natural fiber composites computed with Mori-Tanaka Method.

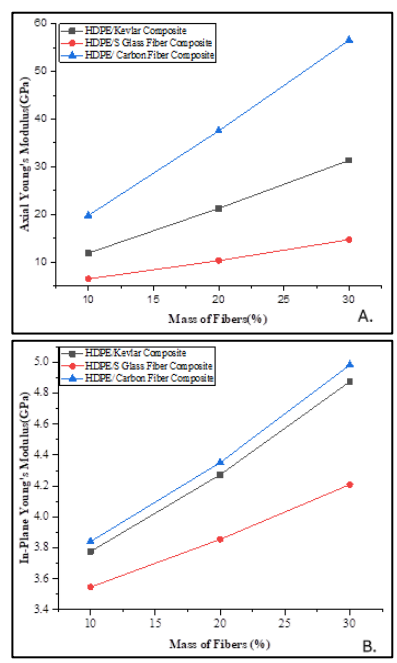

Figure 5: Comparison of (A) axial Young's modulus and (B) In-plane Young's modulus for different synthetic fiber composites computed with Mori-Tanaka method.

2.6 *Modelling of impact analysis*

There is an extensive amount of research available regarding impact assessments on material plates. These works have made understanding the dynamic and temporal response of the structures under varied stress circumstances possible. Studies have revealed that a number of factors, some of which are mentioned below, have a significant impact on how these structures respond.

- The characteristics of the material include Young's modulus of the impactor (E_i) and the plate (E_c), the density of the impactor (ρ_i) and the plate (ρ_c), and the friction coefficient between the impactor and the plate.
- Geometric features include the impactor's radius (R_i), form, and plate dimensions.
- Boundary conditions: Support location, impactor velocity (V_i), and impact location.

Depending on the previously described factors, impacts can be categorized into multiple groups [26]. A sufficiently high impactor velocity has the potential to cause significant structural deflections. These strikes are classified as high velocity impacts and frequently result in perforation and damage. Ballistic impacts are impacts with extremely high velocities that are frequently used in aerospace and military applications [27]. Conversely, as proposed by Richardson *et. al*., low-velocity impacts are those in which the stress distribution is unaffected by the stress wave traveling over the material's width [28]. This suggests that an impact can be classified as low-velocity if its duration is greater than the time it takes for the stress wave to propagate through the material's thickness. The lowest eigenmode will control the deformation in a low-velocity impact if the impactor mass (M_i) is similar to the structure's mass.

2.6.1 Numerical modeling

The model used in this study is based on a standard electrodynamics equation, specifically Equation (17), which describes the propagation of stress waves. For impact analysis, composite plates with pinned support at the edges are shown in Figure 6. These plates are subjected to impact by a non-deformable hemispherical projectile with a deliberately low velocity to ensure a low-velocity impact state. The surfaces of the plates are assumed to be frictionless, allowing the neglect of frictional force and tangential shear stress resulting from the impact.

The deflection of the plate upon contact is considered as the sum of plate indentation (d) and global displacement (w) from the mean position, as given by Equation (18). The work-energy principle is utilized to derive the governing equations (Equations (19) and (20)) for the impact of the rigid projectile on the composite plate. The equations involve the conservation of momentum (Equation 19), where F_c represents the force due to contact, and the work-energy principle (Equation 20), which accounts for external work and changes in potential energy associated with bending, indentation, and membrane deformation.

$$\frac{\partial \sigma_i}{\partial x_i} + F_i = \rho \frac{\partial u_i}{\partial t^2} \tag{17}$$

$$\delta = d + w \tag{18}$$

$$F_C = \frac{d}{dt}\left(M_i V_{f,i} + M_p V_{f,p} - M_i V_{i,i}\right) \tag{19}$$

$$W_{ext} = \Delta PE = \Delta SE_{bending} + \Delta SE_{indentation} + \Delta SE_{membrane} \tag{20}$$

$$\int_o^\delta F_C . dx = \int_o^w K_{bs} . x . dx + \int_o^w K_m . x^3 . dx + \int_o^d K_c . x^{1.5} . dx \tag{21}$$

The mathematical representation includes terms such as bending and shear stiffness (K_{bs}), which depend on the second moment of area (I), length of the plate (L), and Young's modulus (E_c). The second term in Equation (21) describes the strain energy stored due to membrane deformation, usually negligible for small deformations. The last term represents energy stored due to indentation and is a nonlinear function of beam deflection. The contact stiffness (K_c) is calculated based on the contact law discussed in the subsequent section, along with the pressure response of the plate concerning indentation.

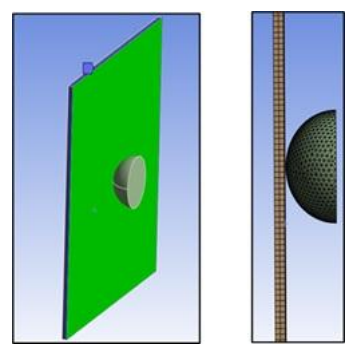

Figure 6: Plate and impactor assembly (left) and half-section view of the plate after impact (right).

2.6.2 Hertz contact law

The Hertz contact law plays a critical role in the simulation of low-velocity impacts, offering a fundamental understanding of the deformation and interaction between two elastic bodies subjected to compressive forces. Specifically relevant in scenarios where the impact duration is relatively prolonged, such as in low-velocity impacts, the Hertz contact law becomes a cornerstone in modeling the contact mechanics between an impacting object and the target material. The law assumes a spherical shape or spheres at the points of contact, simplifying the geometry for mathematical treatment. It facilitates the calculation of parameters such as the depth of penetration and the contact area, considering material properties like Young's modulus, Poisson's ratio, and the radius of curvature of the contacting bodies. Notably, the law assumes elastic deformation, wherein materials return to their original shape after the load is removed. Within this model, the Hertz contact law is integrated to predict deformation and stress distribution during the impact event. The model involves this by solving equations derived from Hertzian contact theory to determine parameters, such as contact force, indentation depth, and pressure distribution.

2.6.3 Finite element approach to impact analysis

A hemispherical impactor (R_i = 0.05 m) and plate (0.50 ×0.50 × 0.01 m) were modeled using explicit dynamics simulation with a step size of 0.002 s. The impactor had a mass of 10 g and a velocity of 10 m/s, making it noticeably stiff. First-order hexahedral elements were utilized to mesh the plate, and rigid shell elements were used in the impactor. The simulation was done for four different natural fiber composites with fibers of ramie, hemp, jute, and flax, and three synthetic fiber composites with fibers of S glass, Kevlar, and carbon in the matrix of HDPE. The fiber percentage was varied between 10% to 30%. The performance of all the composites was compared for the displacement, induced stress, and force absorption characteristics. All the composites undergoing the study were considered to be transversely isotropic. Ansys Workbench was used to perform the FE analysis for the current study. The workflow used for the modeling and simulation is depicted in Figure 7, and the details pertaining to the mesh are shown in Table 4.

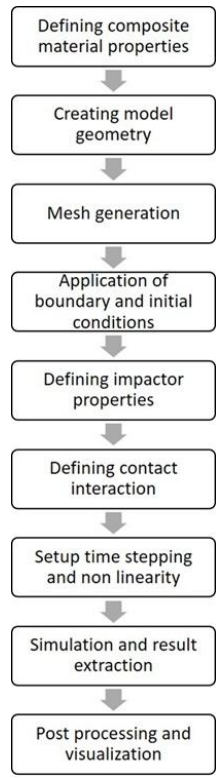

Figure 7: Workflow used for low-velocity impact analysis of composite materials.

Table 4: Mesh details.

Property	Value
Element shape	Hexahedral
Number of elements	3075 (8-node hexahedral) 300 (6-node wedge)
Seed size	0.2
Meshing technique	Sweep

A mesh convergence analysis was conducted by refining the plate seed size (0.25 to 0.10) and observing the peak contact force and maximum mid-span displacement. Convergence was deemed appropriate when both measurements differed by less than 3% between consecutive refinements. According to this criterion, the production mesh utilized first-order hexahedral elements for the plate and a rigid hemispherical impactor.

Edges were modeled as simply supported in a solid formulation by restricting out-of-plane displacement (w = 0) along all four edges while permitting in-plane movement; two corner nodes were marginally limited in-plane to mitigate rigid-body motion. A frictionless contact was established between the rigid hemispherical impactor and the plate. The mass of the impactor and its beginning velocity were

established at 10 g and 10 m/s, respectively. The composite laminae were regarded as transversely isotropic, with stiffness matrices constructed from Mori-Tanaka-derived engineering constants.

3 Results and Discussion

This section compares and discusses the low-velocity impact outcomes for all natural and synthetic fibers. The mechanical performance of natural fibers, including jute, flax, hemp, and ramie, was assessed using measures such as force reaction, deformation, and induced stress for fiber mass percentages of 10%, 20%, and 30%, as shown in Figure 8. At 10% mass fraction, jute had the maximum force reaction of about 1.5 kN, outperforming other natural fibers like flax, which peaked at 0.6 kN. However, as the mass fraction grew to 20%, jute's force reaction declined dramatically to 0.25 kN, representing an 83% reduction, whereas hemp achieved a peak of 2 kN. Increasing the mass fraction to 30% continued this pattern, with flax and hemp experiencing 90% and 87.5% reductions, respectively, while jute's force reaction increased by around 440%. In comparison, ramie regularly showed a 700% increase in force reaction, rising from 0.25 kN at 10% to 2.0 kN at 30%, demonstrating its better reinforcing capabilities. Deformation reduced as the fiber concentration increased, indicating that the composites were stiffer. Flax showed the least deformation at a mass fraction of 10%, followed by ramie at 20% and flax and hemp at 30%. These findings highlight the important impact of fiber composition on mechanical characteristics in composite materials.

Ramie's consistent increase in force reaction indicates its promise as a steady and dependable reinforcement material. Ramie's exceptional mechanical properties are due to its molecular and structural features. Ramie fibers, which are predominantly made up of cellulose microfibrils embedded in a matrix of hemicellulose and lignin, have intrinsic stiffness and strength that are required to sustain increasing stresses as the mass fraction increases in composites [29]. Ramie fibers have an extremely high tensile strength and load-bearing capability due to their robust, linked network of cellulose chains bound together by hydrogen bonds. Furthermore, ramie's efficient interfacial bonding with the composite matrix improves load transfer efficiency and lowers the danger of fiber-matrix debonding under stress, ensuring structural integrity [30]. As the mass fraction of ramie fibers increases, their larger volume within the composite allows for better dispersion of applied pressures, reducing localized stress concentrations and assuring more uniform force reactions throughout different mass fractions [31]. Furthermore, ramie's low coefficient of thermal expansion and low moisture absorption contribute to its outstanding dimensional stability, which ensures constant mechanical performance with time. These combined characteristics establish ramie as a dependable and high-performance natural fiber choice in composite materials, particularly for applications that require predictable mechanical qualities and endurance.

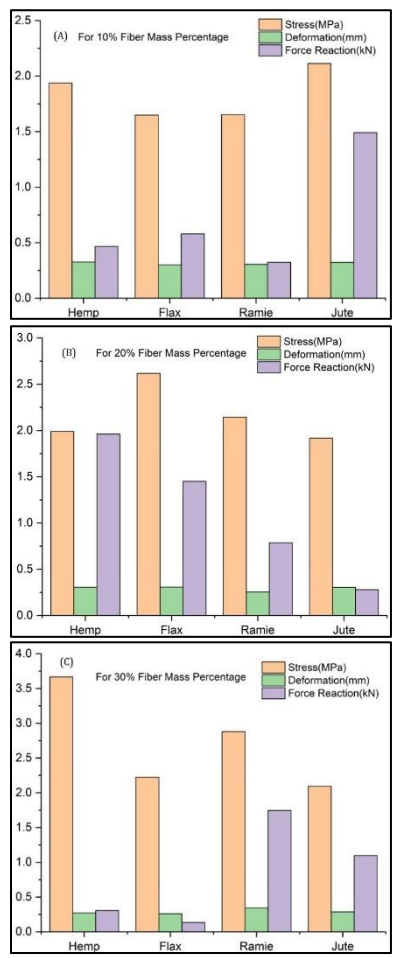

Figure 8: Comparison of HDPE base natural fiber composites for (A) 10 %, (B) 20 % and (C) 30 % mass percentage of fibers under low velocity impact for stress, deformation, and force reaction.

In contrast, synthetic fibers (Kevlar, glass fiber, and carbon fiber) display unique patterns in deformation, force reaction, and produced stress with varying mass fractions, as illustrated in Figure 9. carbon fiber maintained a stable force reaction of 0.45 kN at 10% and 20%, with a minor increase to 0.75 kN at 30%, resulting in a 66.7% gain across the examined range. This homogeneity was reflected in the stress response, which increased from 2 MPa to 4 MPa between 10% and 20%, although deformation remained the lowest among synthetic fibers at greater mass fractions. Kevlar showed a significant 100% rise in stress from 20% to 30%, demonstrating a higher sensitivity to fiber content. Glass fiber showed mild fluctuations in force reaction and stress, indicating a silica-based composition and intermediate stiffness.

These diverse behaviors result from basic variations in the molecular structures and properties of Kevlar, glass fiber, and carbon fiber. Carbon fiber's robust rigidity and strength are due to its strong carbon-carbon bonding, which allows it to maintain similar mechanical properties across different mass fractions [32]. In contrast, Kevlar's aromatic polyamide structure provides excellent tensile strength and impact resistance, but its stress behavior suggests that intermolecular interactions within the composite matrix may vary as fiber concentration increases [33]. Glass fibers, mostly made of silica (SiO_2), provide rigidity and resilience to heat and chemicals. Their mechanical behavior under changing mass fractions is typically reflective of their composition and structural properties, with moderate fluctuations in performance [34].

The composites' low-velocity impact response also indicated the presence of localized damage phenomena. Stress concentrations were more pronounced around the site of impact in natural fiber systems with lower stiffness, such as jute and flax, at higher mass fractions. This resulted in localized matrix yielding and potential interfacial debonding. Conversely, ramie/HDPE composites demonstrated a more consistent stress transfer, which mitigated localized failures and led to a more consistent increase in force reaction. The higher modulus of synthetic fibers, such as carbon fiber, resulted in minimal localized damage, which in turn restricted matrix deformation and distributed stresses more equitably. Kevlar, in contrast, demonstrated localized shear banding at higher mass fractions, which is consistent with its energy-absorbing properties. Despite the absence of progressive damage models in this investigation, the findings indicate that the quality of interfacial bonding, the distribution of stress within the matrix, and the rigidity of natural fibers are all significant factors in the development of localized failure.

The comparative research indicates that natural fibers such as ramie have a high potential to replace certain synthetic fibers, particularly glass fiber, in applications requiring stiffness, impact resistance, and thermal stability, particularly in the automotive and construction industries. Despite its environmental benefits, ramie cannot yet match the exceptional stiffness, tensile strength, and fatigue resistance of carbon fiber, which is still used in aerospace, high-performance automotive, and sports applications due to its lightweight durability and dependable performance in extreme conditions.

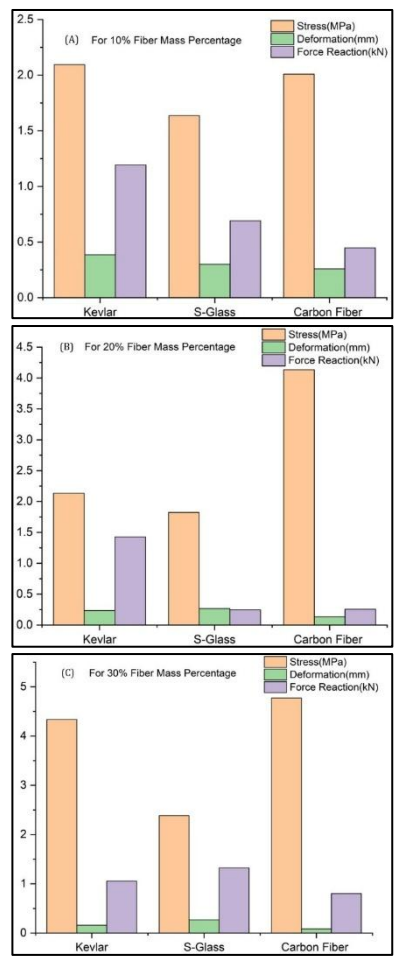

Figure 9: Comparison of HDPE base synthetic fiber composites for (A) 10 %, (B) 20 % and (C) 30 % mass percentage of fibers under low velocity impact for stress, deformation, and force reaction.

4 Conclusions

This research developed and validated a computational–experimental framework to evaluate the low-velocity impact performance of natural and synthetic fiber composites within an HDPE matrix. Microwave-assisted compression-molded HDPE/ramie composites were fabricated and tensile-tested, with experimental elastic moduli showing close agreement with Mori–Tanaka predictions (mean error ≈ 9.4%). This validation supports multiscale homogenization for predicting properties of other fiber-reinforced HDPE composites and ensures reliable transfer of data into finite element impact simulations. Results revealed that ramie/HDPE composites exhibited a steady 700% increase in force response with fiber content, highlighting strong reinforcement potential. In contrast, jute composites showed highly inconsistent behavior, while flax and hemp suffered major performance declines at higher fractions. Carbon fiber composites maintained stable growth in impact response with minimal deformation, underscoring their suitability for high-performance uses.

The study also identified limitations, including reliance on linear elastic models without progressive damage criteria, assumptions of a rigid impactor and frictionless contact, and neglect of environmental influences such as temperature and moisture, which reduce generalizability. Future work should explore fatigue and cyclic impact, environmental durability, and advanced finite element approaches incorporating cohesive damage models. Integrating these with uncertainty quantification and life-cycle assessment will provide a more holistic understanding of the sustainability and performance of natural fibers as alternatives to synthetic reinforcements.

Acknowledgments

We extend our sincere thanks to Navrachana University for funding the current research.

Author Contributions

R.S.: conceptualization, methodology reviewing and editing; N.J.: investigation, data analysis, writing an original draft. All authors have read and agreed to the published version of the manuscript.

Conflicts of Interest

The authors declare no conflict of interest.

References

[1] S. Siengchin, "A review on lightweight materials for defence applications: Present and future developments," vol. 24, pp. 1–17, 2023, doi: 10.1016/j.dt.2023.02.025.

[2] P. S. Bisht, G. Arora, and H. Pathak, "Strain-rate sensitivity analysis of microwave processed polypropylene-carbon nanotube composites," *Journal of Engineering Research*, In press, Apr. 2024, doi: 10.1016/j.jer.2024.04.022.

[3] G. Arora, "Experimental analysis of blended nanocomposites processed using compression molded microwave process," *Proceedings of the Institution of Mechanical Engineers, Part N: Journal of Nanomaterials, Nanoengineering and Nanosystems*, 2024, doi: 10.1177/23977914231224054.

[4] V. Salomoni, G. Mazzucco, C. Pellegrino, and C. Majorana, "Three-dimensional modelling of bond behaviour between concrete and FRP reinforcement," *Engineering Computations (Swansea, Wales)*, vol. 28, no. 1, 2011, doi: 10.1108/02644401111096993.

[5] S. K. Palaniappan, M. K. Singh, S. M. Rangappa, and S. Siengchin, "Eco-friendly biocomposites: A step towards achieving sustainable development goals," vol. 17, no. 4, 2024, doi: 10.14416/j.asep.2024.02.003.

[6] A. S. Bhatnagar, A. Gupta, G. Arora, S. Padmanabhan, and R. G. Burela, "Mean-field homogenization coupled low-velocity impact analysis of nano fibre reinforced composites," *Materials Today Communications*, vol. 26, 2021, Art. no. 102089, doi: 10.1016/j.mtcomm.2021.102089.

[7] G. O. Shah and G. Arora, "Nanostructured composites: Modelling for tailored industrial application," *Applied Science and Engineering Progress*, vol. 17, no. 4, Aug. 2024, Art. no. 7519, doi: 10.14416/j.asep.2024.08.004.

[8] M. K. Singh, R. Tewari, S. Zafar, S. M. Rangappa, and S. Siengchin, "A comprehensive review of various factors for application feasibility of natural fiber-reinforced polymer composites," *Results in Materials*, vol. 17, p. 100355, Mar. 2023, doi: 10.1016/j.rinma.2022.100355.

[9] T. L. S. Ming, E. Jayamani, S. K. Heng, H. PVS, and J. Subramanian, "The effects of microwave curing on dielectric properties of banana fiber reinforced high-Density polyethylene composite,"

Applied Science and Engineering Progress, vol. 17, no. 4, Aug. 2024, Art. no. 7530, doi: 10.14416/j.asep.2024.08.012.

[10] M. K. Gupta and R. K. Srivastava, "Tensile and flexural properties of sisal fibre reinforced epoxy composite: A comparison between unidirectional and mat form of fibres," *Procedia Materials Science*, vol. 5, 2014, doi: 10.1016/j.mspro.2014.07.489.

[11] P. Sahu and M. K. Gupta, "Sisal (Agave sisalana) fibre and its polymer-based composites: A review on current developments," *Journal of Reinforced Plastics and Composites*, vol. 36, no. 24, 2017, doi: 10.1177/0731684417725584.

[12] J. A. Suba and S. K. Boominathan, "Acoustic, mechanical and thermal properties of Luffa/Jute fiber-reinforced bio-composites," *Applied Science and Engineering Progress*, vol. 17, no. 4, Aug. 2024, Art. no. 7526, doi: 10.14416/j.asep.2024.08.006.

[13] S. B. Nagaraju, S. Sudhakar, P. S. R. S. Reddy, S. S. Seshadri, and G. Arora, "Mechanical characterization and water absorption behavior of waste coconut leaf stalk fiber reinforced hybrid polymer composite: Impact of chemical treatment," *Applied Science and Engineering Progress*, vol. 17, no. 3, May 2024, Art. no. 7371, doi: 10.14416/j.asep.2024.05.003.

[14] R. V. Sevak, A. Gupta, and R. G. Burela, "Microwave-aided fabrication of natural fiber hybrid composites: A synergistic approach to mechanical, wear, and computational property analysis," *Proceedings of the Institution of Mechanical Engineers, Part J: Journal of Engineering Tribology*, vol. 239, no. 9, pp. 1163–1182, Sep. 2025, doi: 10.1177/13506501251350832.

[15] V. Yadav and S. Singh, "A comprehensive review of natural fiber composites: Applications, processing techniques and properties," *Materials Today: Proceedings*, vol. 56, pp. 2537–2542, 2022, doi: 10.1016/j.matpr.2021.09.009.

[16] T. Guleria, N. Verma, S. Zafar, and V. Jain, "Fabrication of Kevlar®-reinforced ultra-high molecular weight polyethylene composite through microwave-assisted compression molding for body armor applications," *Journal of Reinforced Plastics and Composites*, vol. 40, no. 7–8, pp. 307–320, Apr. 2021, doi: 10.1177/0731684420959449.

[17] S. C. Her and S. J. Liu, "Analytical model for predicting the interfacial stresses of carbon nanotubes-reinforced nanocomposites," *Engineering Computations (Swansea, Wales)*, vol. 31, no. 2, pp. 353–364, 2014, doi: 10.1108/EC-01-2013-0014.

[18] S. Kilikevičius, S. Kvietkaitė, K. Žukienė, M. Omastová, A. Aniskevich, and D. Zeleniakienė, "Numerical investigation of the mechanical properties of a novel hybrid polymer composite reinforced with graphene and MXene nanosheets," *Computational Materials Science*, vol. 174, 2020, Art. no. 109497, doi: 10.1016/j.commatsci.2019.109497.

[19] R. Ishraaq, S. M. Nahid, S. Chhetri, O. Gautam, and A. M. Afsar, "A molecular dynamics investigation for predicting the optimum fiber radius and the effect of various parameters on the mechanical properties of carbon nanotube reinforced iron composite," *Computational Materials Science*, vol. 174, 2020, Art. no. 109486, doi: 10.1016/j.commatsci.2019.109486.

[20] W. Hufenbach, M. Gude, C. Ebert, M. Zscheyge, and A. Hornig, "Strain rate dependent low velocity impact response of layerwise 3D-reinforced composite structures," *International Journal of Impact Engineering*, vol. 38, no. 5, pp. 358–368, 2011, doi: 10.1016/j.ijimpeng.2010.12.004.

[21] Y. Zhu and Y. Sun, "Dynamic response of foam core sandwich panel with composite facesheets during low-velocity impact and penetration," *International Journal of Impact Engineering*, vol. 139, p. 103508, 2020, doi: 10.1016/j.ijimpeng.2020.103508.

[22] K. J. Narayana and R. Gupta Burela, "A review of recent research on multifunctional composite materials and structures with their applications," in *Materials Today: Proceedings*, vol. 5, pp. 5580–5590, 2018, doi: 10.1016/j.matpr.2017.12.149.

[23] T. Mori and K. Tanaka, "Average stress in matrix and average elastic energy of materials with misfitting inclusions," *Acta Metallurgica*, vol. 21, no. 5, pp. 571–574, May 1973, doi: 10.1016/0001-6160(73)90064-3.

[24] M. Mohammed et al., "Interfacial bonding mechanisms of natural fibre-matrix composites: An overview," *Bioresources*, vol. 17, no. 4, pp. 7031–7090, 2022, doi: 10.15376/BIORES.17.4.MOHAMMED.

[25] I. Elfaleh et al., "A comprehensive review of natural fibers and their composites: An eco-friendly alternative to conventional materials," *Results in Engineering*, vol. 19, p. 101271, 2023, doi: 10.1016/j.rineng.2023.101271.

[26] G. B. Chai and S. Zhu, "A review of low-velocity impact on sandwich structures," *Proceedings of the Institution of Mechanical Engineers, Part L: Journal of Materials: Design and Applications*, vol. 225, no. 4, pp. 207–230, Oct. 2011, doi: 10.1177/1464420711409985.

[27] J. J. Andrew, S. M. Srinivasan, A. Arockiarajan, and H. N. Dhakal, "Parameters influencing the impact response of fiber-reinforced polymer matrix composite materials: A critical review," *Composite Structures*, vol. 224, p. 111007, Sep. 2019, doi: 10.1016/j.compstruct.2019.111007.

[28] M. O. W. Richardson and M. J. Wisheart, "Review of low-velocity impact properties of composite materials," *Composites Part A: Applied Science and Manufacturing*, vol. 27, no. 12, pp. 1123–1131, 1996, doi: 10.1016/1359-835X(96)00074-7.

[29] R. V. Sevak, R. G. Burela, G. Arora, and A. Gupta, "Microwave-assisted fabrication of high-strength natural fiber hybrid composites for sustainable applications: An experimental and computational study," *Proceedings of the Institution of Mechanical Engineers, Part L: Journal of Materials: Design and Applications*, vol. 239, no. 5, pp. 898–909, Aug. 2024, doi: 10.1177/14644207241269567.

[30] C. Chen et al., "Comparative analysis of natural fiber reinforced polymer and carbon fiber reinforced polymer in strengthening of reinforced concrete beams," *Journal of Cleaner Production*, vol. 263, p. 121572, Aug. 2020, doi: 10.1016/j.jclepro.2020.121572.

[31] N. T. Tuli, S. Khatun, and A. B. Rashid, "Unlocking the future of precision manufacturing: A comprehensive exploration of 3D printing with fiber-reinforced composites in aerospace, automotive, medical, and consumer industries," *Heliyon*, vol. 10, no. 5, p. e27328, Mar. 2024, doi: 10.1016/j.heliyon.2024.e27328.

[32] B. A. Newcomb, "Processing, structure, and properties of carbon fibers," *Composites Part A: Applied Science and Manufacturing*, vol. 91, pp. 262–282, Dec. 2016, doi: 10.1016/j.compositesa.2016.10.018.

[33] Y. Zhou, J. Hou, X. Gong, and D. Yang, "Hybrid panels from woven Kevlar® and Dyneema® fabrics against ballistic impact with wearing flexibility," *The Journal of The Textile Institute*, vol. 109, no. 8, pp. 1027–1034, Aug. 2018, doi: 10.1080/00405000.2017.1398122.

[34] R. Velmurugan and V. Manikandan, "Mechanical properties of palmyra/glass fiber hybrid composites," *Composites Part A: Applied Science and Manufacturing*, vol. 38, no. 10, pp. 2216–2226, Oct. 2007, doi: 10.1016/j.compositesa.2007.06.006.